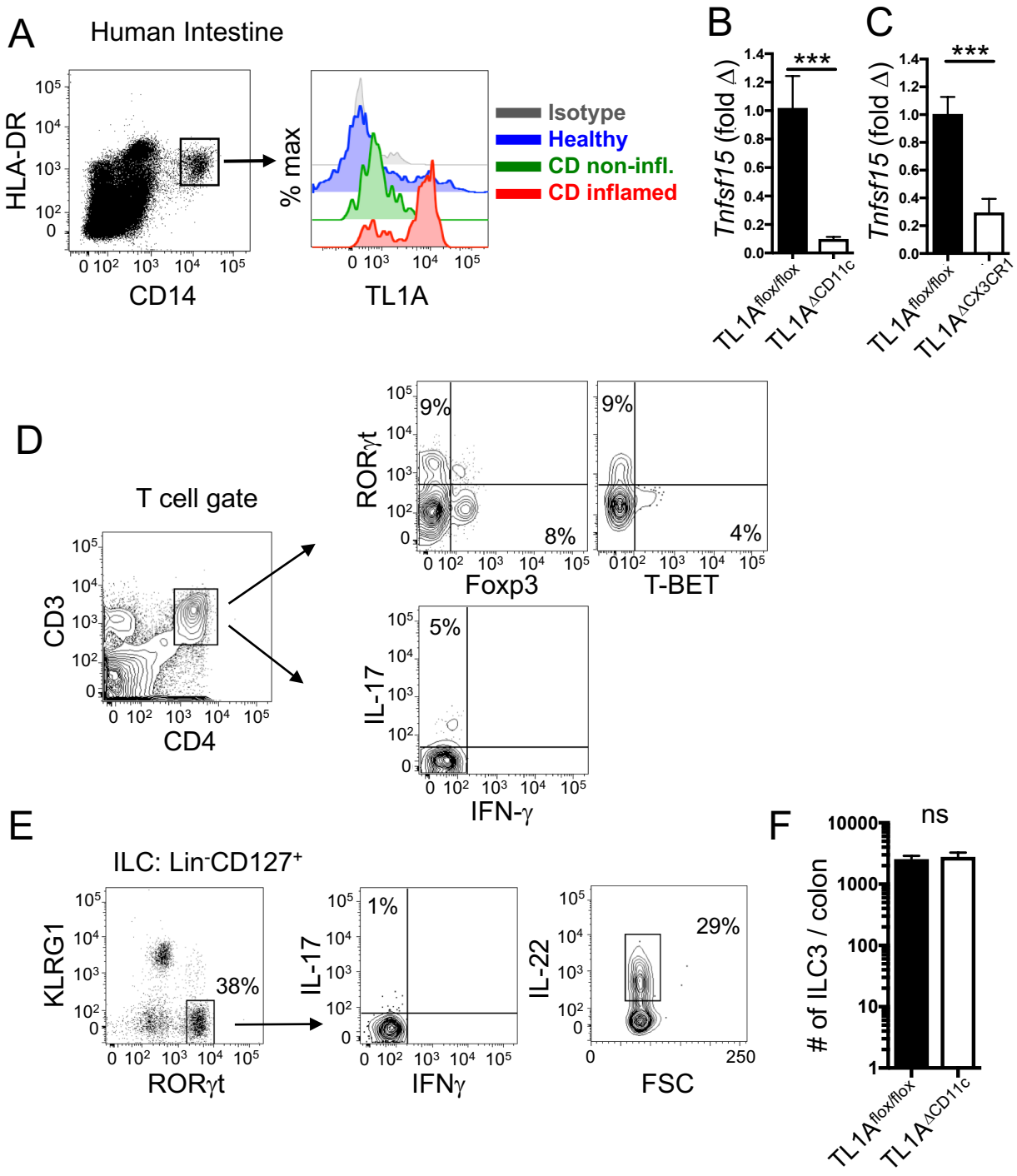

Figure. S1. MNP-derived TL1A in human Crohn's disease and the immune response in mouse models of colitis, Related to Figure 1. Legend on next page

Figure S1. MNP-derived TL1A in human Crohn's disease and the immune response in mouse models of colitis, Related to Figure 1. (A) $CD14^+$ $HLA\text{-}DR^+$ MNPs were identified from human intestinal biopsies by flow cytometry and TL1A surface expression is shown. One representative sample from Figure 1B is shown. **(B)** *Tnfsf15* expression from FACS-sorted $MHCII^+CD11c^+$ MNPs from *Tnfsf15*$^{flox/flox}$ *Itgax-cre* (called $TL1A^{flox/flox}$) or *Tnfsf15*$^{flox/flox}$ *Itgax-cre* (called $TL1A^{\Delta CD11c}$) littermate mice was determined by qPCR. (**C**) qPCR of *Tnfsf15* expression in $MHCII^+CD11c^+CD11b^+$ MNPs from 4OHT-treated *Tnfsf15*$^{flox/flox}$ *Cx3cr1-creER* (called $TL1A^{\Delta CX3CR1}$) and *Tnfsf15*$^{flox/flox}$ (called $TL1A^{flox/flox}$) littermate mice. N = 3-4 mice group. (**D**) Representative $CD3^+CD4^+$ T cell gating for cytokine and transcription factor analysis shown in Figure 1G. (**E**) Representative Lin^-CD127^+ ILC3 gating for cytokine and transcription factor analysis shown in Figure 1H. (**F**) Total number of ILC3 per colon in (N = 5 mice/group). Data in (B), (C), and (F) are mean ± s.e.m and were analyzed by two-tailed Student's t-test. ***P<0.001.

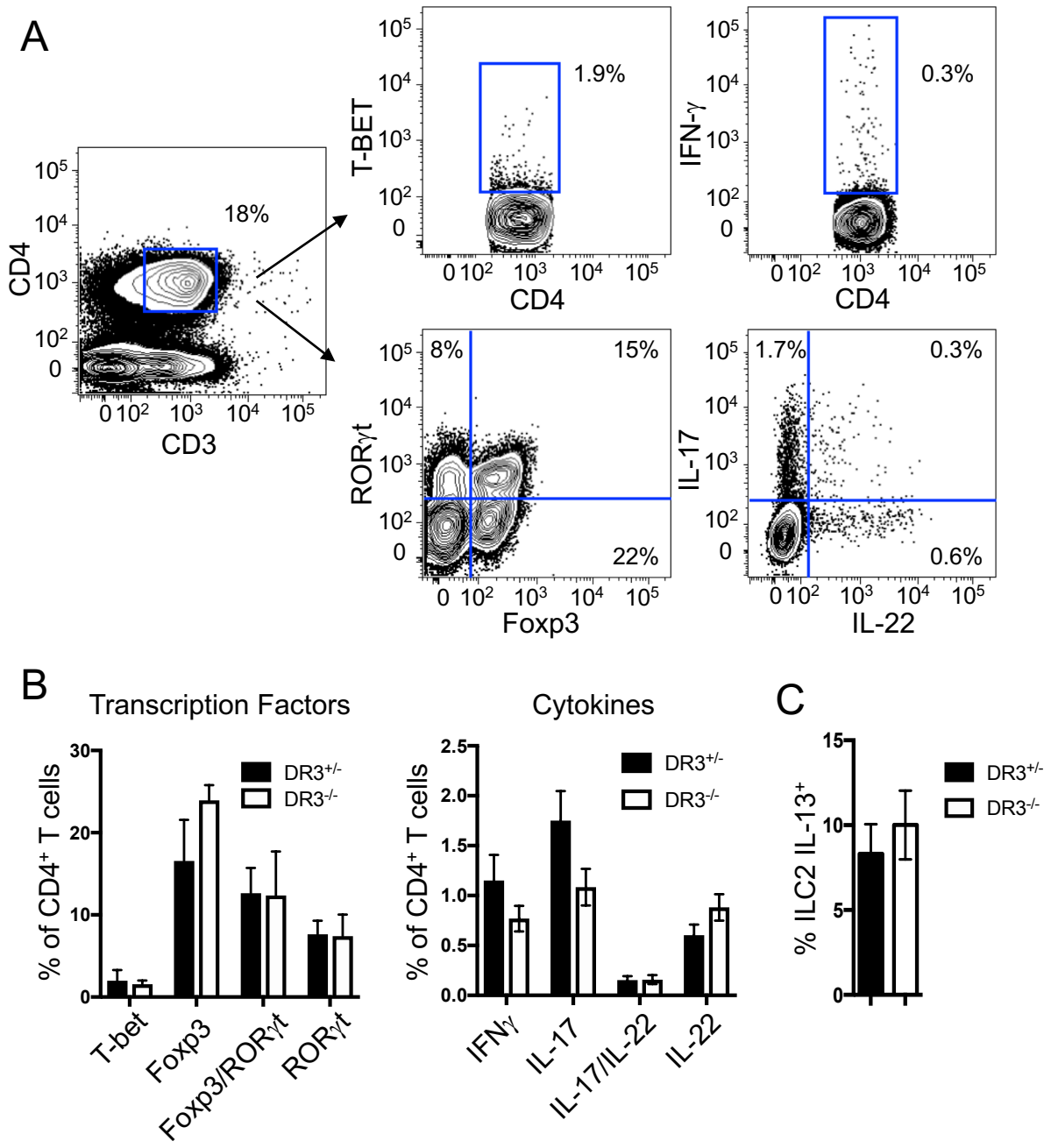

Figure S2. CD4⁺ T cell and ILC2 response in DR3-deficient mice, Related to Figure 3. (**A**) Representative gating of CD4⁺ T cells and intracellular transcription factor and cytokine staining (**B**) Percentage of colonic Foxp3⁺,RORγt⁺, or T-BET⁺ T cells (N=4 mice/group) or IFNγ, IL-17, or IL-22 producing T cells (N = 8 mice/group) from DSS-treated DR3$^{+/-}$ and DR3$^{-/-}$ littermate mice 9 days after starting DSS treatment. (**C**) Percentage of colonic Lin^{-}CD127⁺KLRG1⁺GATA3⁺ ILC2s producing IL-13 from DSS-treated DR3$^{+/-}$ and DR3$^{-/-}$ littermate mice 9 days after starting DSS treatment (n = 5-6 mice/group). Data in (B) and (C) show mean ± SEM. Data are compiled from two independent experiments.

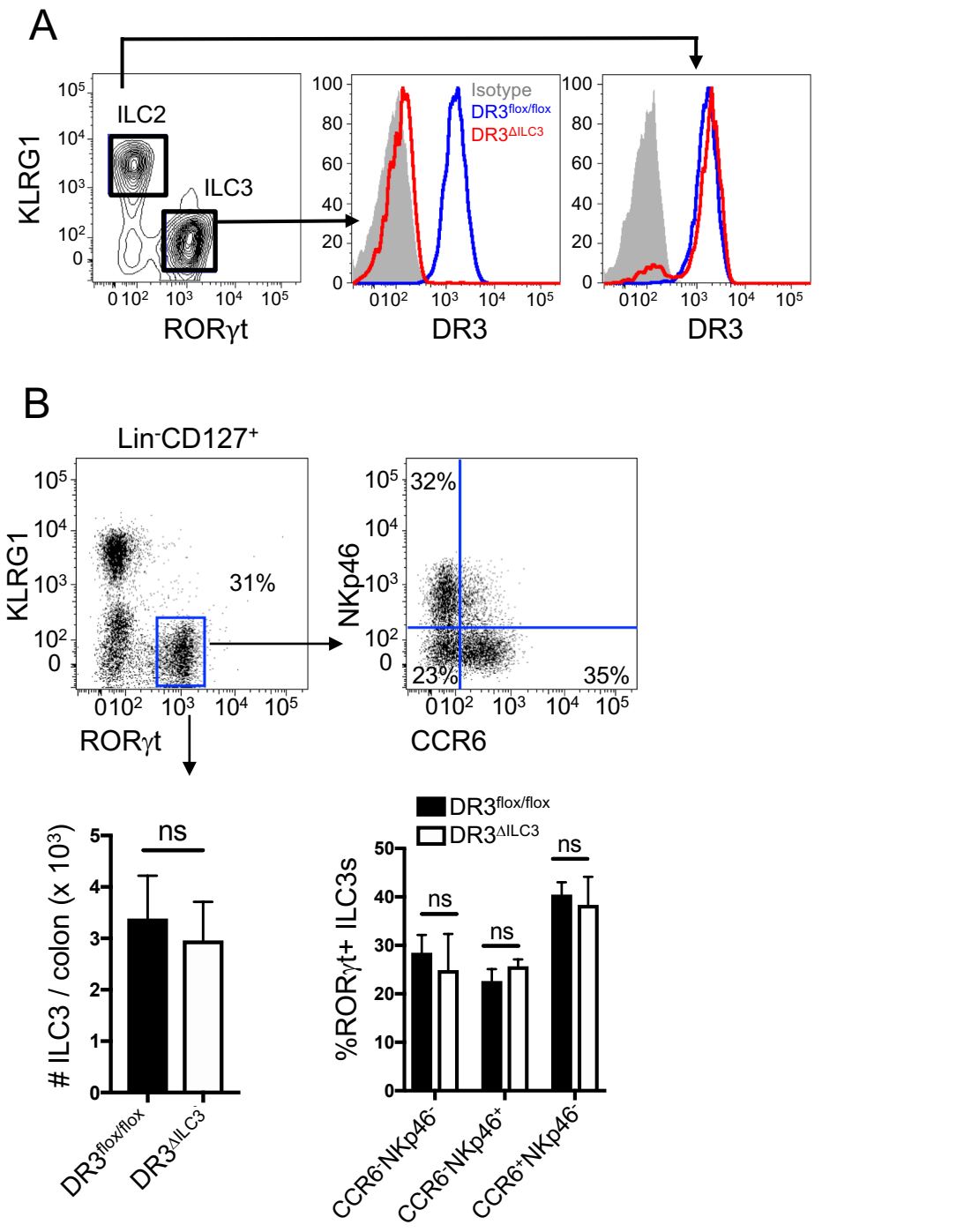

Figure S3. ILC3-specific deletion of DR3 does not impact ILC3 number or subsets, Related to Figure 3. (**A**) Representative flow cytometry analysis of extracellular DR3 expression on *Tnfrsf25*$^{flox/flox}$ *RAG2*$^{-/-}$ (called DR3$^{flox/flox}$) and *Tnfrsf25*$^{flox/flox}$ *Rorc-cre RAG2*$^{-/-}$ (called DR3$^{\Delta ILC3}$). (**B**) Gating of colonic Lin^{-}CD127^{+}RORγt^{+} ILC3s and surface staining for NKp46 and CCR6 subtypes is shown. Total number of ILC3 / colon is shown and percentage of ILC3 subtype in DR3$^{flox/flox}$ and DR3$^{\Delta ILC3}$ littermate. One of two experiments is shown with N = 5 mice/group. Data are mean ± SEM.

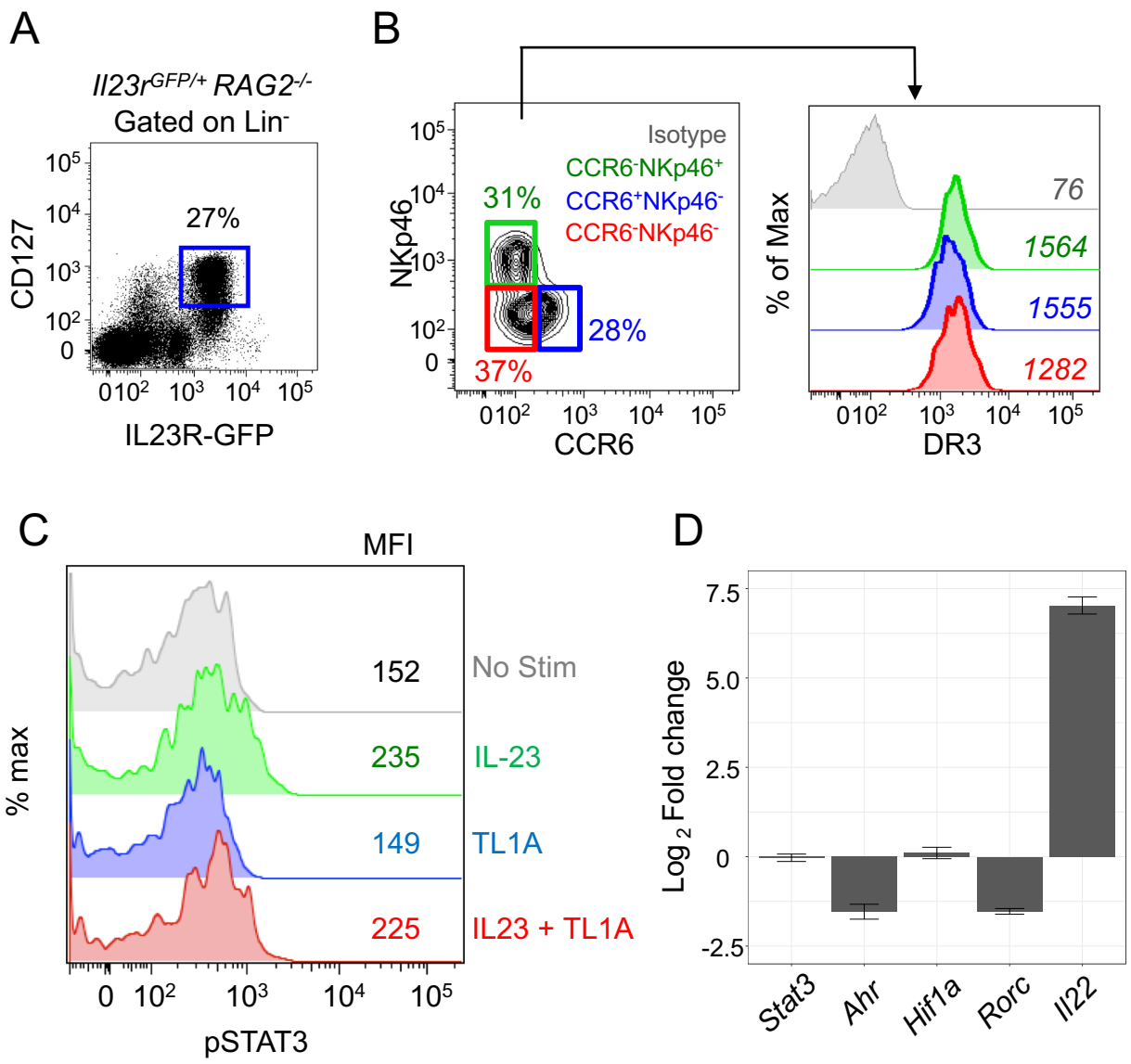

Figure S4. TL1A stimulation regulates ILC3 production of IL-22, Related to Figure 4. **(A)** Sorted from *Il23r*$^{GFP/WT}$ *RAG2*$^{-/-}$ reporter mice (Lin$^-$: CD3$^-$CD5$^-$CD19$^-$CD11b$^-$TCRγδ$^-$KLRG$^-$). (**B**) ILC3 (Lin$^-$CD127$^+$IL23R-GFP$^+$) subsets were evaluated for extracellular DR3 expression by flow cytometric analysis. (**C**) Sorted ILC3s were stimulated with IL-23 and/or TL1A and intracellular phosphoflow was performed 30 minutes after stimulation. The histogram indicates the MFI of the plot. One of two representative experiments is shown. (**D**) RNA sequencing was performed on unstimulated or rTL1A-stimulated sorted ILC3s. The mean fold change of key transcription factors and Il22 is shown. Data are compiled from two independent experiments. Error bars indicate the log standard error.

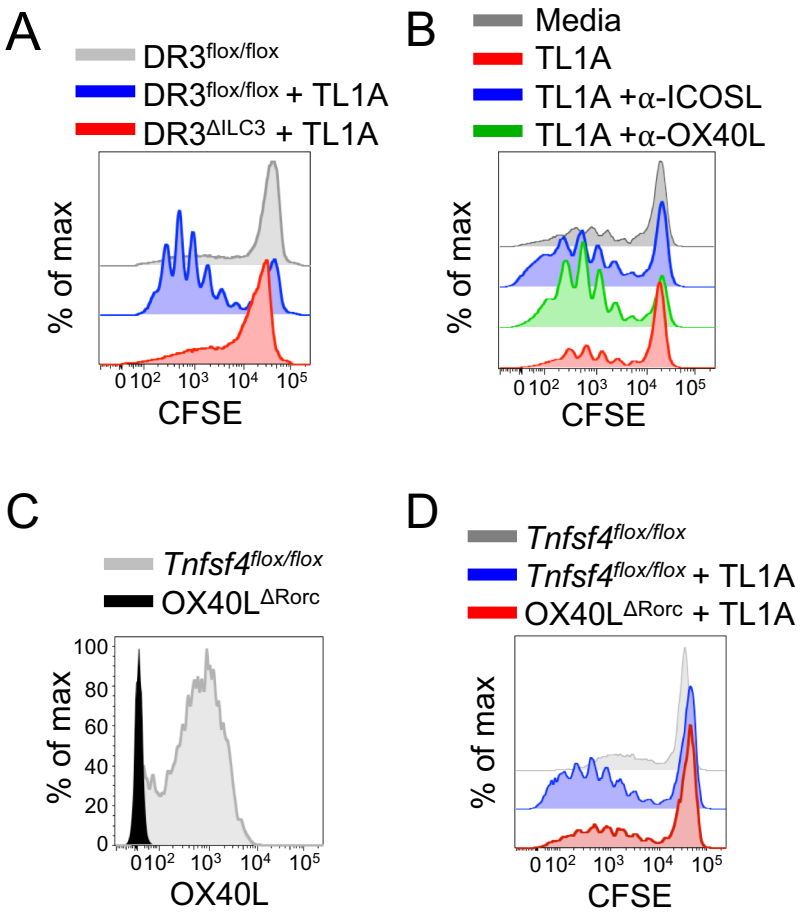

Fig. S5. ILC3 co-stimulation of T-cells is DR3- and OX40L-dependent, Related to Figure 5. (**A,B**) Sort-purified, CFSE-labeled naïve CD4$^+$ T-cells from OT-II transgenic mice were cultured for 6 days with sort-purified MHCII$^+$ ILC3 loaded with OVA peptide from either (A) *Tnfrsf25*$^{flox/flox}$ *RAG2*$^{-/-}$ (called DR3$^{flox/flox}$) or *Tnfrsf25*$^{flox/flox}$ *Rorc-cre RAG2*$^{-/-}$ (called DR3$^{\Delta ILC3}$) mice with or without rTL1A, as indicated or (B) WT mice with or without rTL1A and the indicated neutralizing antibodies. One representative of three independent experiments is shown. (**C**) Lin$^-$CD127$^+$ ILC3 cells were sort-purified from *Tnfsf4*$^{flox/flox}$ and *Tnfsf4*$^{flox/flox}$ *Rorc-cre* (called OX40L$^{\Delta Rorc}$) littermate mice and extracellular OX40L levels were measured by flow cytometry after 18h stimulation *ex vivo* with rTL1A. (**D**) Sort-purified, CFSE-labeled naïve CD4$^+$ T-cells from OT-II transgenic mice were cultured for 6 days with sort-purified MHCII$^+$ ILC3 from either *Tnfsf4*$^{flox/flox}$ or OX40L$^{\Delta Rorc}$ mice with OVA peptide and rTL1A, as indicated. One representative of two independent experiments is shown.

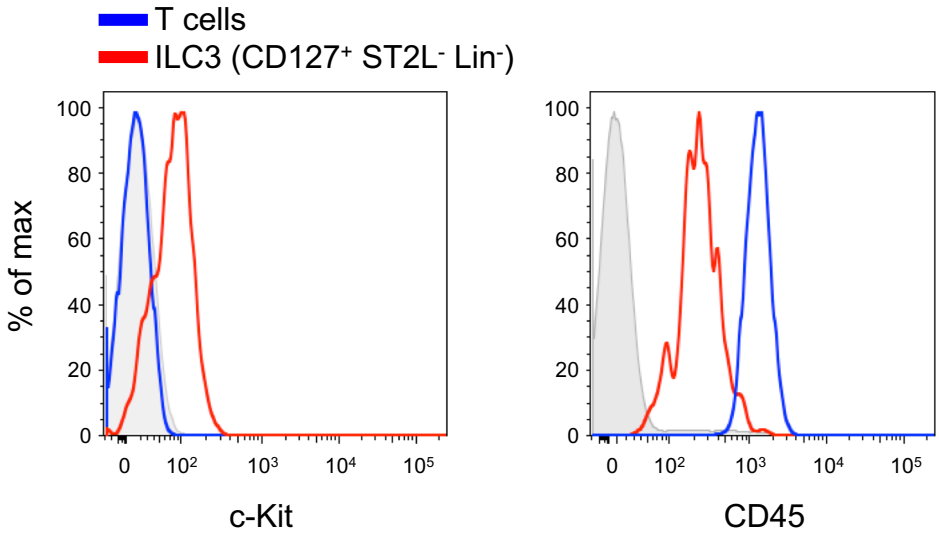

Figure S6. C-Kit and CD45 intermediate surface staining in human intestinal CD127$^+$ Lineage$^-$ ILCs, Related to Figure 6. C-Kit and CD45 surface staining of CD127$^+$ ST2L$^-$ Lin$^-$ human intestinal ILCs compared to CD3$^+$ T cell (blue) or unstained control (grey). One representative plot of data shown in Figure 6C is displayed.

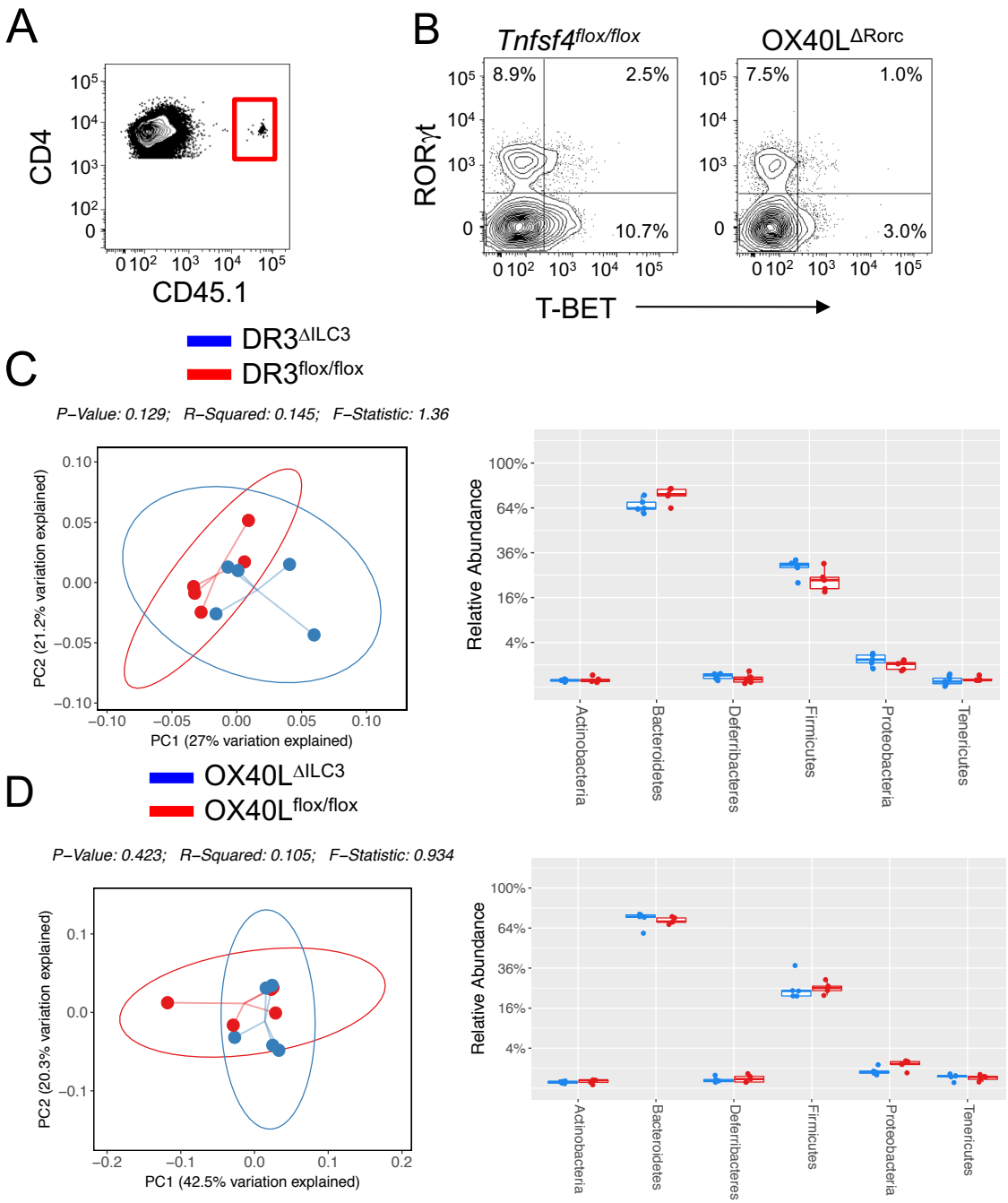

Figure S7. CD4⁺ T cell analysis in OX40L$^{\Delta ILC3}$ mice and the intestinal microbiome of DR3- and OX40L-deficient mice compared to littermate controls, Related to Figure 7.

Figure S7. CD4$^+$ T cell analysis in OX40L$^{\Delta ILC3}$ mice and the intestinal microbiome of DR3- and OX40L-deficient mice compared to littermate controls, Related to Figure 7. (A) Flow cytometric analysis of CD45.1$^+$ CD3$^+$CD4$^+$Vα2$^+$ OTII T-cells following transfer of naïve CD45.1$^+$ CD3$^+$CD4$^+$Vα2$^+$ OTII T-cells into CD45.2$^+$ *Tnfsf4*$^{flox/flox}$ or CD45.2$^+$ *Tnfsf4*$^{flox/flox}$ *Rorc-cre* (called OX40L$^{\Delta Rorc}$) mice in Figure 7A. (**B**) Flow cytometric analysis of intranuclear RORγt and T-BET in CD4$^+$ T cells from intestinal lamina propria of OX40L$^{flox/flox}$ and OX40L$^{\Delta Rorc}$ littermate mice shown in Figure 7B. (**C,D**) 16S rRNA analysis was performed for microbiome analysis. Principal coordinate analysis using the Sorensen dissimilarity matrix (left) and relative abundance (right) are shown at the phylum level for (C) *Tnfrsf25*$^{flox/flox}$ *RAG2*$^{-/-}$ (called DR3$^{flox/flox}$, N=5*)* and *Tnfrsf25*$^{flox/flox}$ *Rorc-cre RAG2*$^{-/-}$ (called DR3$^{\Delta ILC3}$, N=5) and (D) *Tnfsf4*$^{flox/flox}$ *RAG2*$^{-/-}$ (called OX40L$^{flox/flox}$, N=5) and *Tnfsf4*$^{flox/flox}$ *Rorc-cre RAG2*$^{-/-}$ (called OX40L$^{\Delta ILC3}$, N=5).